Available online www.jocpr.com

Journal of Chemical and Pharmaceutical Research, 2016, 8(8):758-771

Research Article

ISSN : 0975-7384
CODEN(USA) : JCPRC5

Biologically Synthesized Quercetin Loaded Magnetite Nanoparticles Enhanced Cytotoxicity and Radiosensitivity of Cancer Cells *in Vitro*

S. A. Elmasry[1], M. A. Elgawish[2], *O. E. El-Shawy[3], M. A. Askar[1,2], E. A. Helmy[4] and L. A. Rashed[5]

[1]*Molecular Biology Department, Genetic Engineering and Biotechnology Research Institute, Sadat City-Egypt*
[2]*Radiation Biology Research Department, National Center for Radiation Research and Technology (NCRRT), Atomic Energy Authority (AEA), Cairo, Egypt*
[3]*Health and radiation Research Department, NCRRT, AEA, Cairo, Egypt*
[4]*Regional Centre of Mycology and Biotechnology (RCMB), Al-Azhar University, Cairo, Egypt*
[5]*Medical Biochemistry Department, Faculty of Medicine, Cairo University, Cairo, Egypt*

ABSTRACT

Fe_3O_4 nanoparticles (MNPs) have great advantages in cancer applications due to their unique structure and strong magnetic properties. In this study, the formulated quercetin (Q) loaded MNPs were mediated by Aspergillus oryazae. $FeSO_4$ used as a substrate to prepare MNPs in a single step, co-friendly biological method. UV– Visible spectrophotometer, X-ray diffraction, Fourier transform infrared analysis and Transmission electron microscopy were used to study the morphology and structure of the formulated MNPs as well as QMNPs. The cytotoxicity of the formulated NPs was examined against different human cancer cells. The enhancement of the most sensitive cancer cells in response to radiation therapy (RT) by QMNPs was demonstrated via several cytotoxicity assays including cell survival, intracellular ROS levels, early DNA damage and cell apoptosis in sub G1 phase and cell cycle distribution were measured with MTT assay, Electron Spin Resonance (ESR) Spectroscopy, flow cytometry analysis, respectively to evaluate the biocompatibility of the formulated the nano-structure. The results revealed that Q was loaded on the surface of the prepared MNPs to obtain QMNPs suggesting that ferric ions are located in globular nanoparticles chelated by quercetin. The formulated NPs were amorphous with size ranging from 40 to 60 nm. Biological investigations displayed that QMNPs was concentration dependent and cell specific cytotoxicity with IC50 values of 11nM/ml, 75.4 nM/ml and 104 nM /ml for MCF-7, HepG2 and A459 cell lines respectively. QMNPs also, appeared to be a potent enhancer for radiation treatment as evidenced by the increased radiosensitivity of MCF-7 cells in comparison with RT alone.

Key words: cancer cell lines, Magnetite-Quercetin Nanoparticles, Radio-Sensitivity, Targeted-Drug Delivery, anticancer agents.

INTRODUCTION

According to the World Health Organization (WHO), ~ 1.3 million women are diagnosed with breast cancer each year [1]. In Egypt, the incidence of breast cancer represented 25% of all newly diagnosed malignancies [2]. Radiotherapy (RT) is commonly used in cancer therapy either alone or in conjunction with surgery and/or chemotherapy. Since X- and γ-rays result in lethal alterations of the tumor at the subcellular level [3], the preservation of the surrounding healthy tissue remains a challenge. The use of radiosensitizers has been suggested for achieving this issue [4]. Thus, radiosensitizers cold identified as therapeutic or inert agents that enhance the effects of radiation therapy. They are composed of heavy elements with a tendency to absorb ionizing radiation and can be exploited for preferentially depositing a high dose in the tumor area [5-6] while a significantly lower dose is absorbed in the surrounding healthy tissue [7]. Moreover the interaction between the radiosensitizers and the

ionizing beam produces a shower of secondary elemental particles (photons and electrons) [8-9] which produce highly reactive radicals [10]. These reactive radicals react with water (the main component of the cells) and oxygen resulting in the interruption of the activity of biomolecules in adjacent of the tumor site [11]. The preferential dose deposition in the tumor and the resulting biomolecular alterations can therefore lead to the death of cancerous cells [12].

Reports of the literature emphasized that adjuvant therapies in combination with RT are more likely to increase the overall effectiveness of radiotherapy in patients with breast cancer and caused better survival. The use of radiosensitization agents is one of the ways to enhance the radiation treatment outcome [13]. Irradiation kills cancer cells by inducing DNA damage and generation of ROS which in turn leads to the damage of the biomolecules [14]. Besides, the accumulation of ROS can deregulate the apoptotic signaling pathway, ultimately inducing apoptosis [15-17]. Since most of radiosensitizers can upregulate ROS which considered as a potential target for improving RT [18-19]. In recent years, naturally occurring dietary compounds or daily food ingredients have received greater attention and brings a new hope in the field of cancer prevention and treatment research due to their safety and lack of discernible toxicity to normal cells. This alternative approach has been used to treat a wide spectrum of cancers [20].

Quercetin (3,5,7,3′,4′-pentahydroxy flavone) represents the most abundant dietary flavonoid found in a broad range of fruits, vegetables and beverages, with antioxidant and anti-inflammatory properties have been associated with the prevention, inhibiting and reversing the progression of cancer [21-22]. Several reports have been suggested that Quercetin is able to inhibit the growth of tumor cells, prevent cancer metastasis and suppress cancer cell proliferation by inducing tumor cell apoptosis or cell cycle arrest at a certain stage within the cycle, suggesting that the compound has potential for use in the treatment of cancer [23-25]. Literature studies demonstrated that combination of quercetin with radiotherapy can enhance tumor radiosensitivity both in vitro and in vivo. However, therapeutic applications of quercetin have been restricted to oral administration due to its sparing solubility in water and instability in physiological medium [26-27]**.** In order to overcome these issues, an efficient drug delivery system should be formulated based on the naturally available adjuvant therapeutic agents.

The nanoparticles (NPs) have been attracted lot of consideration as a drug targeted and delivery system to allow the administration of the required therapeutic active compound concentration at the tumor site for a convenient period of time [28] at a controlled and sustained rate to the site of action and to increase therapeutic benefit, while minimizing side effects [29]. Chemical and physical methods for the synthesis of nanoparticles are the common approaches, but their use is limited because they are costly and harmful to the environment. The biogenic synthesis is, therefore, the best choice. In this methods the biological systems such as bacteria, fungi, plants were used to transform the organic metal into metal nanoparticles via the reactive capacity of proteins and metabolites present in these organisms [30]. The use of fungi in the green synthesis of metal nanoparticles has been reported [31]. Since fungi contain enzymes and proteins as reducing agents and can be invariably used for the synthesis of metal nanoparticles from their salts. Since some fungi are pathogenic, one has to be cautious while working with them during experiment [32].

Nanoparticles (NPs) have unique characteristics like small particle size, large surface area, and the capability of changing their surface properties. Therefore they have several advantages over other delivery system [33]. Additionally, it has been proven that NP-based drug delivery systems assure passive (size-based targeting due to their size up to ~100 nm) as well active targeting (surface funtionalization by targeting ligand) and enhanced therapeutic efficacy of anticancer agents [34]. NPs possess good biocompatibility, they can restrict the bio-distribution profile and target the drug to the tumor regions, which increases therapeutic efficiency and reduces nonspecific toxicity of anticancer drugs [35].

Magnetite nanoparticles (MNPs) constitute an important class of nanomaterials widely studied for their potential use as a targeted drug delivery in biomedicine fields [36-37]. The physicochemical properties of quercetin loaded MNPs confirmed their utility as anticancer agent for drug delivery applications [38]. Magnetic nanoparticles have been emphasized as a new drug delivery system to control quercetin releasing for breast cancer therapy [39]**.** The use of Fe3O4NPs as nanocarriers for drug delivery has been reported. Gallo and co-workers substantiate that the concentration of magnetic microspheres containing drug in the brain was 100-400 higher than its level when taken in a solution dosage form [40] indicating the success of magnetic particles as a drug delivery. Moreover, the encapsulated quercetin on the dextran coated Fe3O4 nano-carriers was testified as one of the potential techniques to get rid the mentioned problems and it enhance the drug's bioavailability. The quercetin entrapped polymeric micelles (PEG-OCL) also, has an excellent solubility and inhibits the growth of cancer cells via inducing cell cycle arrest in G2/M phase [41].

In the present research quercetin loaded magnetic NPs was formulated using magnetite Fe_3O_4. The magnetite Fe_3O_4 was synthesized biologically by using simple precipitated method and mediated for the first time by Aspergillus *Oryazae using* $FeSO_4$ as a substrate to yield Fe3O4 NPs.

Thus, we intended to conduct this study to characterize the formulated QMNPs to be used as a new drug delivery system for adjuvant cancer therapy into tumor with demonstration of its antitumor activity in human cancer cells and its efficacy to enhance the tumor radiosensitivity *in vitro*, with a focus on assessing the critical mechanisms involved in this antitumor and radiosensitizing activities.

EXPERIMENTAL SECTION

Biological Synthesis and Characterization of Quercetin-Magnetite Nanoparticles (QMNPs):

Microorganisms

Aspergillus oryzae fungus was kindly provided by the culture collection unit of the Regional Center for Mycology and Biotechnology (RCMB) Al-Azhar University, Cairo-Egypt. The fungal isolate was sub-cultured and maintained on Sabouraud's Glucose agar (SGA) medium containing (g/l); glucose–20; peptone–10; agar–20 and distilled water,1000 ml; at temperature of 25 (±2)°C and the pH was adjusted at 5.4 ± 0.2.

Biomass production

The biomass of the extract of the fungus was prepared according to the method previously described [42]. The fungus was grown aerobically in a liquid medium containing (g/l) KH_2PO_4–7.0; K_2HPO_4–2.0; $MgSO_4$–0.1; $(NH_4)_2SO_4$–1.0; yeast extract–0.6; and glucose–10.0 and the pH was adjusted at 6.2 ± 0.2. The flasks were inoculated and incubated on orbital shaker at 25°C and agitated at 150 rpm. The biomass was harvested after 72 h of growth by sieving through Whatmann filter paper no.1 followed by extensive washing with distilled water to remove any component from the biomass.

Biological synthesis of magnetite Nanoparticles (MNPs)

In the present study, MNPs were prepared by using FeSO4 as a substrate and mediated biologically by *Aspergillus oryzae*. At 1st the extracellular bioextract of the fungal was prepared for biosynthesis of Fe3O4. For this purpose, 20 g of fresh clean fungal biomass was brought in contact with 100 ml of deionized water in an Erlenmeyer flask and incubated at 25°C in dark shaking incubator (150 rpm) for 72 h. After incubation period, the cell filtrate was obtained by passing it through Whatmann filter paper no.1. Secondly, for synthesis of the MNPs by using FeSO4 as a substrate, 100 ml of cell free water extract of A.*oryzae were* exposed to 10 mM $FeSO_4$ aqueous solutions at (pH 3.1) in 500 ml Erlenmeyer flasks and kept on a shaker (200 rpm) at 27^0C. The reaction was carried out for a period of 120 h in place of the iron cyanide complexes of the earlier experiment. All of The bio-transformed nano-products were centrifuged at 10,000 rpm for 15 min, following which the pellet was re-dispersed in sterile distilled water to dispose of any uncoordinated biological molecules. The process of centrifugation and re-dispersion was run in sterile distilled water and repeated three times to ensure better separation of free entities from the metal nanoparticles. The purified pellets were then sonicated for 30 min using ultrasonicator (united Jeveriy tools supplies, Italy) for more disparity. Finally samples were freeze dried using a lyophilizer (Thermo Electron Corporation, Micro Modulyo 230 freeze dryer). The lyophilized powder was ready for further analysis and characterization.

Characterization of Magnetite (Fe_3o_4) and Quercetin-Magnetite Nanoparticles

Characterization of the prepared MNPs and QMNPs were carried out by different instruments and techniques, including, visual observation, UV– Visible spectrophotometer, X-ray diffraction (XRD) of TEM, Fourier transform infrared (FT-IR) analysis and TEM.

UV–visible spectrophotometric analysis

The qualitative reduction of iron ions for the fungal biosynthesis of MNPs and QMNPs was confirmed via testing the supernatant by UV–visible spectrophotometer (Spectronic Milton Roy 1201 UV). The optical density was measured each 10 min from the beginning of incubation process at different wavelength ranging from 200 nm to 500 nm and the relation between the concentration and the absorbance was plotted on a graph.

X-ray diffraction and Transmission Electron Microscopy (TEM) Analysis

MNPs and QMNPs diameter and shape were determined and reported by Transmission Electron Microscopy **(***TEM JEOL 1010, Japan*) and X-ray diffraction (XRD) (XRD/TEM JEOL 1010, Japan). Samples for TEM analysis were prepared by puting a drop of prepared solution onto a conventional carbon coated copper TEM grids (400 meshes, Plano Gmbh, Germany), allowing the drop to dry overnight at room temperature before imaging. X-ray diffraction analyses as well as the TEM images of the samples were obtained using an accelerating voltage of 30 kV and 80 kV, respectively. At least three images of each sample were taken to have a clear representation of its morphology.

Fourier Transform Infra Red (FT-IR) Spectroscopy analysis

The infrared analysis of the resulted MNPs and QM NPs were performed on a Fourier transform infrared (FT-IR) spectrometer (IRPrestige-21®, German) to verify the protein–nanoparticle interaction and to identify the possible biomolecules which are responsible for reduction of Fe^{3+} ion and capping of the bio-reduced nanoparticles synthesized by the fungal cells. Prior to analysis, the sample powder pellets were placed into the sample holder and FT-IR spectra were recorded in the range of 400–4,000 cm^{-1} at a resolution of 4 cm^{-1}.

Biological Activity of Quercetin -Magnetite (Fe_3o_4) Nanoparticles

Cytotoxicity of QMNPs

In the current study he cytotoxicity of the formulated QMNPs was evaluated against three of human cancer cells included Hepatocarcinoma cell line (HepG2), Human breast adenocarcinoma cell line (MCF-7), and Human alveolar adenocarcinoma cell line (A-549), with the determination of IC50 which is the concentration of the tested material that caused 50% death of the cells.

Cell Culture

HepG2, MCF-7 and A-549 were purchased from the tissue culture unit of the Holding Company for Biological Products and Vaccines (VACSERA), Giza, Egypt and supplied through the American Type Culture Collection (ATCC). The cytotoxic effect of QMNPs against these cells was evaluated. Cells were routinely cultured in DMEM (Dulbecco's Modified Eagle's Medium), all media were supplemented with 10% fetal bovine serum (FBS), 2 mM L-glutamine, containing 100 units/ml penicillin G sodium, 100 units/ml streptomycin sulphate and 250 ng/ml amphotericin B. Cells were maintained at sub-confluency at 37ºC in humidified air containing 5% CO_2. For sub-culturing, monolayer cells were harvested after Trypsin /EDTA treatment at 37°C. Cells were used when confluence had reached 75%. Tested sample was diluted in the assay to begin with the indicated concentration. All cell culture material was obtained from Cambrex BioScience (Copenhagen, Denmark). All chemicals were from Sigma/Aldrich, USA. All experiments were repeated three times.

Cell viability assay and estimation of IC_{50}

Reagents preparation:

MTT solution: 5mg/ml of MTT in 0.9%NaCl, acidified isopropanol (0.04 N Hcl in absolute isopropanol).

Procedure:

MTT metabolic assay was applied according to [43] to demonstrate the cytotoxic potential of the engineered QMNPs on the viability of the three human cancer cells mentioned above. The cells were plated separately in 96 well plates at a concentration of 5×10^5 cells/well. After 24 h, cells were washed twice with 100 µL of serum-free medium and starved for an hour at 37°C. After starvation, cells were treated with 20 µl of serial concentrations of the tested material for 48 h at 37° C, in a humidified 5% CO_2 atmosphere. After incubation, media were removed and 40 µl MTT solution / well were added and incubated for an additional 4 h. Spectrophotometrical absorbance of the purple blue formazan dye was measured in a microplate ELISA reader ***(ELx808 Absorbance Reader)*** at 570 nm. The experiment was carried out in triplicates and the average of the viable cells was calculated. A graph was plotted between the percentage of the viable cells and dilution. Data were expressed as the percentage of relative viability compared with the vehicle control.

Calculation

Percentage of relative viability was calculated using the following equation:

[Absorbance of treated cells/ Absorbance of control cells)] X 100

Further, in our study, according to the IC50 value, the most sensitive cells were used for determination of the optimal irradiation dose that causes optimum inhibition of cell proliferation. Then, the radiosensitization of these cell lines by QMNPs was also examined.

QMNPs and enhancement of radiation sensitivity:

Radiation Sensitivity Test and Estimation of the Optimal Irradiation Dose

Radiation sensitivity test was performed to determine the Proliferation of MCF-7 cells under the effect of 4, 6, 8 and 10 Gy γ- irradiation doses using the metabolically active MTT (3-[4,5-dimethylthiazol-2-yl]-2.5-diphenyl tetrazolium bromide) dye cell proliferation kit (Trevigen Inc., Gaithersburg, MD, USA) as per manufacturer's protocol after 24 hr of the initial irradiation exposure. This assay is based on the capacity of cells to reduce 3-(4,5-dimethylthiazol-2yl)-2,5-diphenyltetrazolium bromide to formazan, a purple crystal metabolized by mitochondria that can be easily visualized in the viable cells by inverse optical microscopy.

Briefly, 10^3–10^5 cells/well were loaded in a 96-well plate and irradiated with the different doses gamma rays. After the irradiation the cells were maintained in 5% CO_2 at 37 ºC. Cell viability was evaluated 24 hours after initial irradiation exposure. At the of the incubation period, cells were incubated in MTT (5mg/mL) for 4 hours hrs at 37^0C. The optical density was measured at 570-630 nm in an ELISA reader *(ELx808 Absorbance Reader*) with the solubilization buffer as blank.

The% of cell viability is determined by the following formula:

% of cell viability= [$OD_{570-630}$ of the treated cells / $OD_{570-630}$ of the untreated control set]

QMNPs Sensitize MCF-7 cells to radiation therapy (RT)

In order to estimate the enhancing killing effect of RT to MCF-7 cancer cells by QMNPs, the inhibition of cell proliferation after 24hr of initial treatments was demonstrated by MTT assay. The culture medium of the control set remained without any treatment. For the other treatments the culture media were removed and replaced with the QMNPs at a concentration of 11nM/ml for the sole drug treatment, another two sets were exposed to 6Gy either alone or in combination with the tested nano material (11nM/ml QMNPs+6Gy irradiation). All the experiments incubated for 24hr. Thereafter, MTT assay test was applied to analyze cell proliferation by using 3-(4, 5-dimethylthiazol-2-yl)-2,5-diphenyl tetrazolium bromide. In brief, 20 µL of MTT (5 mg/mL in PBS) was added to each well and samples were incubated for 4 h at 37°C. The MTT solution was removed, and 100 µL detergent reagent was added into each well to dissolve the precipitate. Then, optical density of the wells was measured at 570-306 nm and photographs were taken and analyzed with the Nikon (Japan) bright field inverted light microscope. The% of cell viability was determined by the formula given above.

Electron Spin Resonance Spectroscopy analysis for detection of the formulated nanomaterial-mediated generation of reactive oxygen species (ROS):

To analyze whether QMNPs enhances the generation of ROS by RT, ***electron Spin Resonance (ESR) Spectroscopy*** also, known as Electron spin (paramagnetic) resonance (EPR) which is a powerful technique for studying chemical species or materials that have one or more unpaired electrons. ESR detects the absorption of microwave energy, which occurs on transition of unpaired electrons in an applied magnetic field. The amplitude of the ESR signal is proportional to the number of the unpaired electrons present in the sample, allowing quantification of free radicals. ESR measurements were performed at room temperature (24 °C) on a Varian E-109 spectrometer (Stefka et al., 2012) equipped with a Bruker ER 041 XG microwave bridge. The ESR measurements were performed with the following settings: frequency 9.27 GHz, field sweep 8 mT, microwave power 4.9 mW, and modulation amplitude 0.11 mT. The galvinoxyl free radical was used as a scavenging object in ESR radical-scavenging measurements. The stability of its freshly prepared ethanol solution was measured for 30 min, and no significant loss of signal was detected. A loss of signal of about 7% was detected after 24 h. Therefore, the fresh radical solutions were prepared daily. AMFJ solution was added to the freshly prepared galvinoxyl solution in ethanol (c = 0.15 mmol/dm^3) in order to obtain various juice concentrations (0.1, 0.2, 0.5, and 1.0 vol %). The same final concentration of the galvinoxyl radical in all samples (c = 0.12 mmol/dm^3) was obtained by addition of adequate amount of water. The juice solution was quickly mixed with the radical solution in the flask and immediately put into the capillary which was then placed in a standard ESR tube. Depending on the sample concentration, ESR spectra were recorded as a function of time starting from the juice and radical solution contact. Recording intervals were 0.5 min and 1.0 min, depending on the sample activity. The signal intensities of galvinoxyl radicals were calculated by the double integration of ESR spectra, using the EW (EPRWare) Scientific Software Service program and expressed in arbitrary units. The signal intensity of the pure 0.12 mmol/dm^3 galvinoxyl solution, measured just before starting the sample measurement, was taken as the reference signal intensity (I_0) for the reaction time t = 0 min. The normalized signal intensity (I_n) after the reaction time t, expressed as a percentage, was calculated as:

$$\boldsymbol{I_n = (I/I_0) \times 100}$$

Where I is the signal intensity of galvinoxyl radicals in juice solution measured at time t. Each sample was analyzed in triplicate. The results are presented as mean values.

Early Apoptosis and Cell cycle Analysis

MCF-7 cells (1.3×10^5) were seeded in 6-well microplates. Prior to analysis, cells were washed with PBS After incubation for 24 hr with IC_{50} concentration (11nM/ml) of the tested nano-compound. To stain with propidium Iodide (PI), cells were suspended in 425 µl of PBS and 25 µL of propidium iodide (1 mg/mL, Sigma-Aldrich, St. Louis, MO, USA). The cell pellets were then resuspended in 1mg/ml PI/ Triton X-100 staining solution (0.1% Triton X-100 in PBS, 0.2mg/ml of RNase A (Sigma-Aldrich, St. Louis, MO, USA), and incubated on ice for 20 min. The DNA content of 10000 cells was analyzed by FACS Caliber flow cytometery (Becton Dickinson, CA, USA) to

calculate the percentages of cells occupying the different phases of the cell cycle determined by using the Mod Fit LT software (Jhi et al., 2014), samples were run in triplicate and each experiment was repeated three times.

RESULTS AND DISCUSSION

Visual characterization of the formulated MNPs as well as the QMNPs was achieved by observing the color of the *A. oryzae* cell free water extract was a pale yellow before the addition of iron nanoparticles (Figure 1 A), this was changed to a golden brownish color on completion of the reaction with $FeSO_4$ for 28h (Figure 1 B). Later, the color was turned to dark brownish as magnetite (Fe_3O_4)-quercetin forming complex achieved by the time (Figure 1 C).

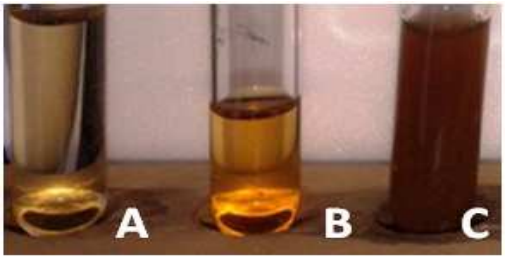

Figure 1. A; The color of the *A.oryzae* cell free water extract, B; Iron nanoparticles with $FeSO_4$ substrate, C; magnetite (Fe_3O_4)-quercetin NPs using $FeSO_4$ as a substrate

***UV-Vis Spectrum Analysis of MNPs and QMNPs*:**

The features of the UV-vis spectrum of the formulated MNPs as well as QMNPs as mediated by *A.oryzae* using the $FeSO_4$ substrate indicated in two curves and illustrated in Figure 2. Two intensive absorption bands of magnetite were observed in curve 1 centered at 360 nm, and 254 nm. In curve 2, two absorption peaks of QMNPs were observed at 256 nm and 377 nm. The absorption peak II of curve 2 was shifted 2 and 17 nm respectively.

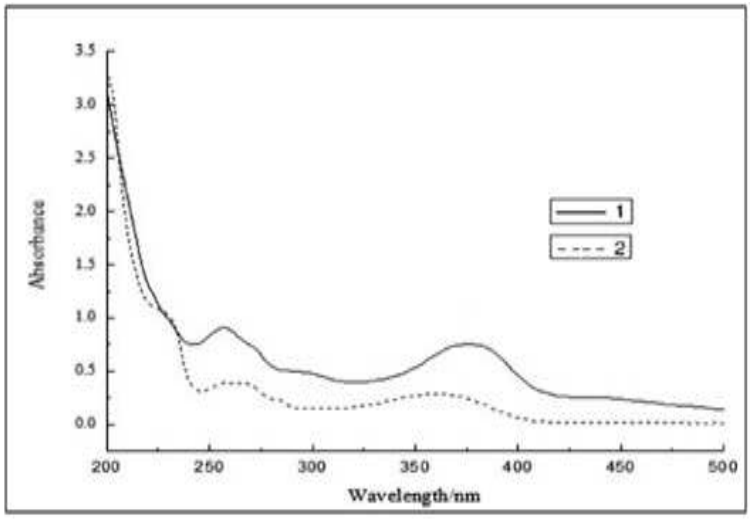

Figure 2. The chromatogram of UV Spectrophotometry of MNPs (curve 1) and QMNPs (curve 2) mediated by A oryzae and FeSO4 as a substrate

Transmission Electron Microscope (TEM) Analysis of MNPs and QMNPs

The size and morphology of our formulated nanoparticles were analyzed with TEM are presented in figure 3. The size of the nanoparticles was measured with the TEM-software analysis system. TEM images showed that the particles were spherical in shape and uniformly distributed (monodispersed) without significant agglomeration. The formulated MNPs were 11 nm in diameter of (fig. 3.A), meanwhile QMNPs were spherical in shape and 40 nm in diameter (fig. 3.B).

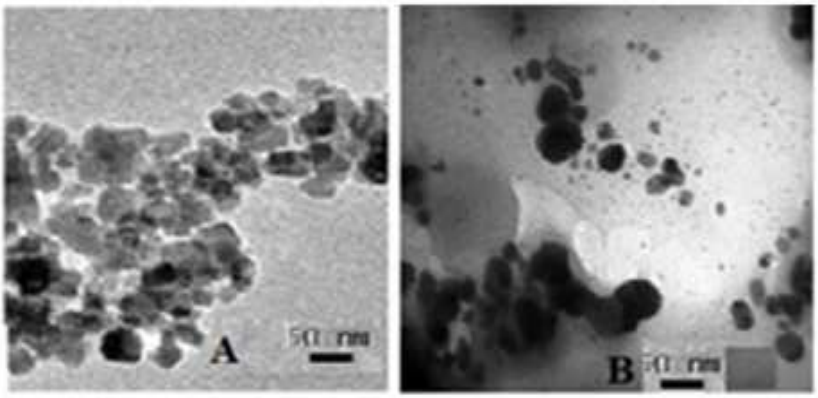

Figure 3: TEM images of the mycosynthesized QMNPs nanoparticle mediated by *A.oryzae* and FeSO4 as a substrate. (A) MNPs and (B) QMNPs. Magnification (X= 200 000k for A and X=100 000K for B)

X-Ray Diffraction Analysis of MNPs and QMNPs

From the XRD image, one can observe diffraction patterns for all samples. The Fe3O4 NPs were pure magnetite (Fe_3O_4) with a cubic inverse spinel structure (Figure 4). The diffraction peaks belong to Fe3O4 NPs prepare by $FeSO_4$ substrate (Figure 4A) were (111); (220); (311); (400); (422); (511); (440), (533); (553). The diffraction peaks belong to QMNPs prepared by $FeSO_4$ substrate were (220) ;(311) ;(400) ;(422); (511); (440) (Figure 4B).

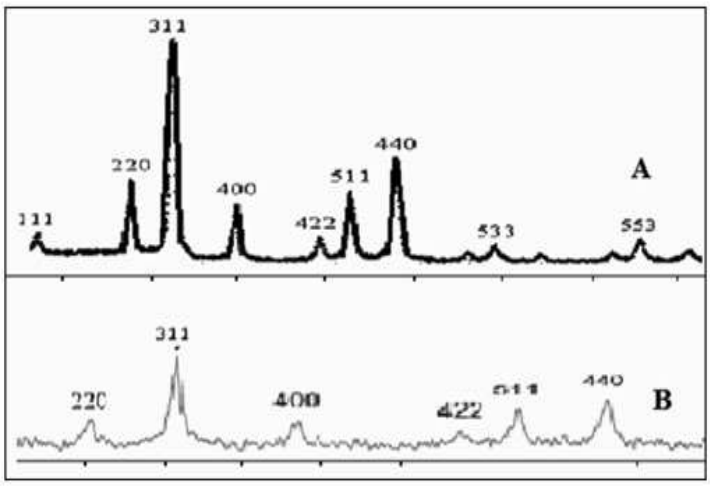

Figure 4: XRD patterns of the mycosynthesized (A) MNPs and (B) QMNPs mediated by A *auyrzae* and $FeSO_4$ as a substrate

Cell viability assay:

The cytotoxic effect of the synthesized QMNPs on the viability of HepG-2, MCF-7 and A459 cancer cells was evaluated *in vitro* after 48 hrs exposure and their IC50 values were determined from a graph of cell viability measured over a range of concentrations from 5- 20 nm/ml in comparison with untreated control cell lines. For this purpose, a line graph was plotted between concentrations (X-axis) versus % inhibition (Y-axis) and then an intersection drawn at 50% inhibition on Y-axis and then correlated to the concentration value on X-axis.

(Figure 5) and (Table 1) showed the percentage of cell viability and the IC50 values after exposure of MCF-7, HepG-2, and A459 cell lines to different concentrations (5, 10,15 and 20 nM/ml) of QMNPs compared to control untreated cells. A significant decrease in the % of viability of MCF-7 cell lines was recorded with IC50 value of 11nM/ml. Meanwhile less cytotoxicity was observed towards HepG-2 with IC50=77.5 nM/ml and A459 with IC50 value of 104nM/ml. Our results clearly suggest that QMNPs exhibited cell specificity and concentration dependant cytotoxicity. Taking into account these data, MCF-7 cell lines and its IC50 value 11 nM/ml of QMNPs were used in the subsequent experiments.

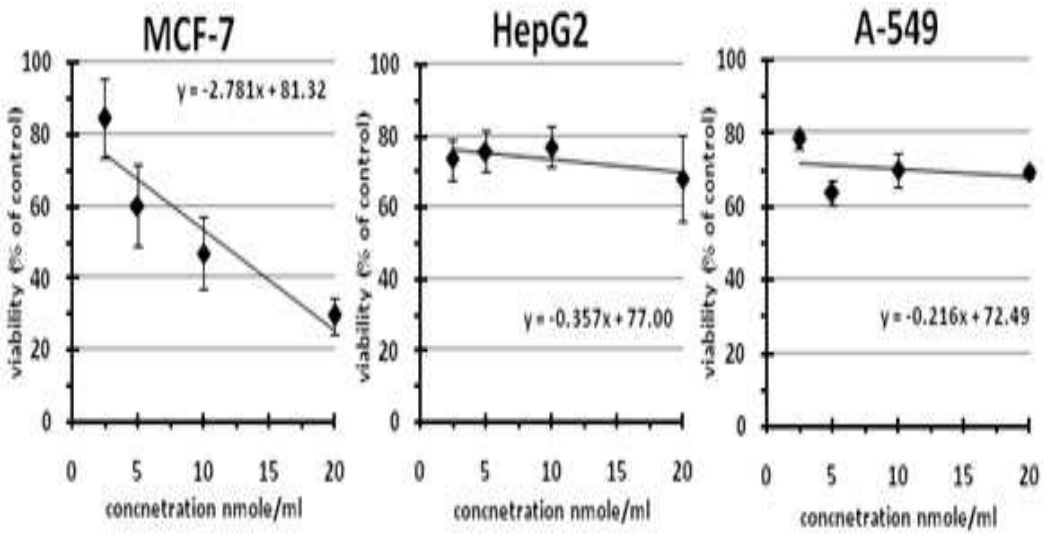

Figure 5: Cytotoxic effect of sample N1 against MCF-7, Hep-G2 and A-549 cells using MTT assay, (n=4). Data expressed as the mean value of cell viability (% of control) ± S.E

Table 1: Comparison between cytotoxicity of QMNPs in different human cell lines after 48 of initial exposure by MTT assay

Cell lines	IC50 (nM/ml)
MCF-7	11.2
HepG-2	77.5
A459	104

Radiation Sensitivity Test and Estimation of the Optimal Irradiation Dose

The MCF-7 cell lines were exposed to different γ-rays doses to demonstrate the optimal radiation dose that cause the optimal inhibition of cell viability using MTT assay. The absorption percentage of treated cells compared to control cells was used to calculate cell viability. Figure 6 revealed that MCF-7 cell lines showed variable degrees of viability after 24h of exposure to the different γ-rays doses. Nevertheless, the greater decrease in the viability of the cells was observed in cells exposed to 6 Gy irradiation dose for 24 hr. The photomicrographs in bright field inverted light microscope associated with the reduction of MCF-7 cells viability after 24 hr of initial exposure to the different irradiation doses as investigated by MTT assay in relation to control untreated MCF-7 cell. As illustrated in (Figure 7), the control cells (A) appeared round, meanwhile B,C,D and E showed formation of formazan crystals with variable degrees of reduction in viability of MCF-7 cell 24 hr post exposure to 4, 6, 8 and 10 Gy respectively. The formation of formazan crystals were more pronounced in 6Gy exposed cells than that of the other sets. These morphological changes were closely correlated with the inhibition of cell proliferation and reduction of the viable cells. Thus the 6Gy irradiation dose was used in subsequent investigations.

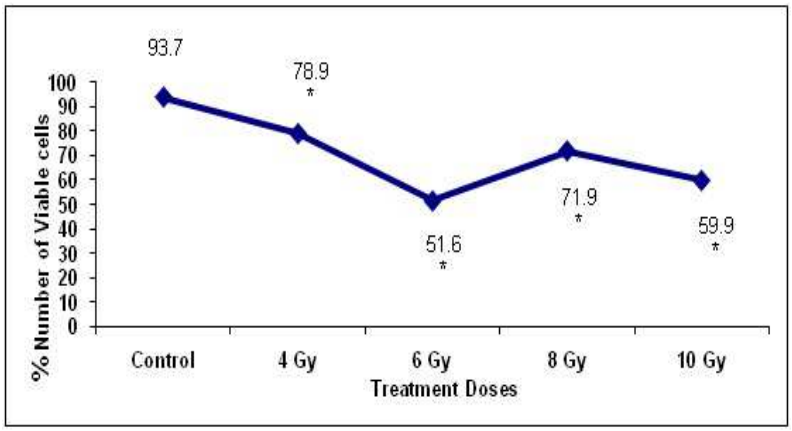

Figure 6: Determination of optimal irradiation dose caused optimal death of MCF-7 cell lines. Each data point was an average of results from three independent experiments performed in triplicate

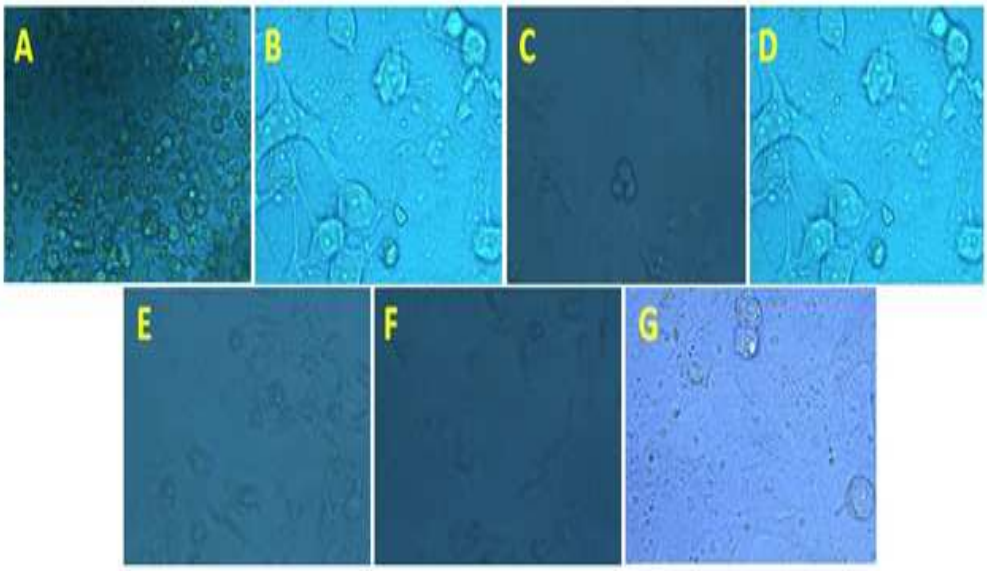

Figure 7: Morphological changes of MCF 7 cell lines qualitatively analyzed by MTT assay. Cells were visualized under inverted light microscope. The photographs (A) represents MCF-7 Control cells and those treated with different doses of gamma irradiation illustrated in (B) treated with 4 Gy, (C) treated with 6 Gy, (D) treated with 8 Gy, (E) treated with 10 Gy 24 hr of the initial irradiation exposure. QMNPs treated cells illustrated in photograph (F) and combined treatment illustrated in photograph (G)

The Potential Effectiveness of QMNPs as Radio Sensitizer

In our investigation, the MTT survival assay was used to determine the enhancement of MCF-7 radiosensitivity by QMNPs. The results showed inhibition of cell survival and proliferation after the sole treatment of QMNPs at a concentration of 11nM/ml to 67.6%. However, combined treatment QMNPs +IR enhanced the killing effect of the 6Gy gamma irradiation as indicated by the great reduction of cells proliferation up to 39.5% comparable with 50.6% reduction post exposure to 6Gy irradiation dose alone and all compared to 93.7 % cells proliferation in the control set (Figure 8).

The morphological changes associated with enhancement of inhibition of MCF-7cell proliferation were analyzed under inverted light microscope. (Figure 7) illustrated the graphs of different treatments. The 6Gy irradiated cells (C); QMNPs treated set (F) and combined treatment (G). The morphological analysis of all groups was investigated in relation to the control set (A). The images C, G & F have distinct morphological apoptotic characteristics such as cell shrinkage with intact membranes as well as condensed cytoplasm along with membrane blebbing which led to the formation of apoptotic bodies compared to the control set (A). It is worth mentioning that these apoptotic characteristic features were more pronounced in the cells received the combinatory treatment (G).

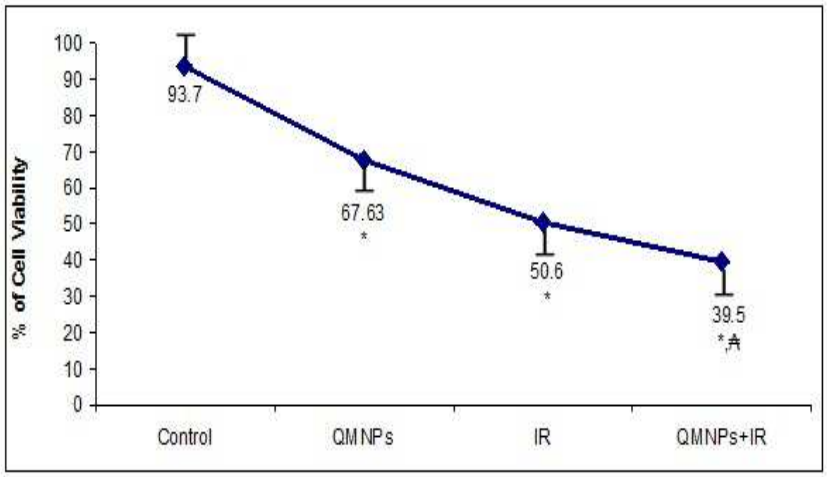

Figure 8: Radiosensitivity of MCF-7 cells treated with 11 nM/ml QM NPs for 24 h prior to exposure to 6Gy of radiation and 24hr post irradiation exposure compared to control cells (non-irradiated MCF-7 cells) and those received the sole irradiation treatment

Detection of ROS generation:

Detection of the intracellular ROS was assessed with the ESR spectroscopy. As shown in (Figure 9), there is a significant elevation (P< 0.05) in the levels of ROS in QMNPs-treated set at a concentration 11nM/ml for 24 hr compared to the level of ROS in control set throughout the experiment. Meanwhile, a high significant (P<0.001) increase was recorded in RT (6 Gy) treated cells post 24 hr of the initial exposure compared with control untreated set. This elevation showed further significant (P<0.0001) increase in the level of ROS after exposure to their combination compared with control untreated cells and (P<0.001) compared with RT treatment alone.

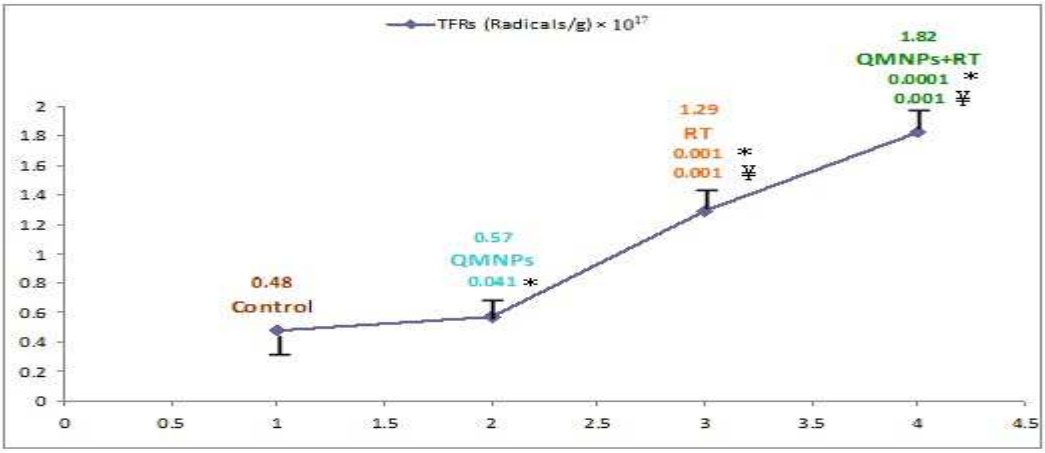

Figure 9: Determination of total free radicals by ESR, * Significant of treated groups from the control set, ¥ Significant from QMNPs+RT from RT set

QMNPs caused early Apoptotic death and altered Cell Cycle Phases

Cell cycle distribution of nuclear DNA was determined through PI staining method followed by Flow-cytometry (FCM) analysis to measure the percentage of sub-G1 populations and distribution of cell fractions in different phases of the cell cycle. In this method the cells were less stained by DNA binding PI dye which is an indicative of early apoptosis that resulted from DNA fragmentation. The cells were accumulated as sub-G1 population peak after losing its DNA. In the present study, as shown in (Figure 10) and (Table 2), 24 hr post QMNPs treatment at concentration of 11.2 nM/ml enhanced the cell population (P<0.001) in sub-G1 phase (16.7%) compared with 1.4% in control untreated cells. whether, QMNPs in combination with RT enhanced the accumulation of cells to 10.4% (P<0.01) compared with 6.2% in RT alone. The increased of cells in sub-G1 suggesting that combined treatment caused serious and irreversible DNA damage and induced early apoptotic cell death. Moreover, the effect of the early damage of DNA was observed in cell cycle progression. The data in (Figure 10) and (Table 2) revealed that QMNPs as sole treatment arrested 47.7% of cell fractions at G1-phase compared to 37.7% in control set. Meanwhile, RT alone arrested 38.9% at G1-phase and 38.1% fractions at S1-phase compared to that of the control. Their combination reduced the cell population in S-phase (24.6%) with increased cell fractions in G1-phase (45.7%). The cells arrested in G1-phase would be induced into apoptosis. Our results suggest that QMNPs enhanced the killing effect of RT in MCF-7 via induction of sub-G1 apoptosis and G1- phase arrest.

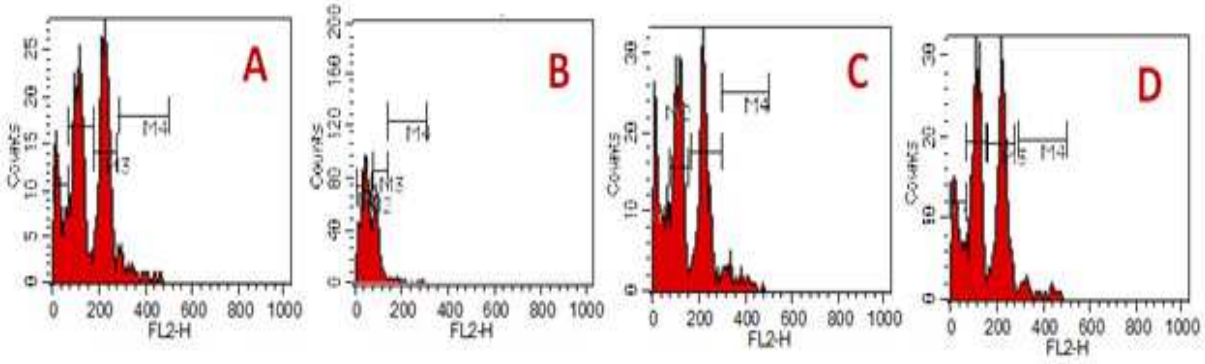

Figure 10: Cell cycle analysis; (A) MCF-7 as control without any treatment, (B) treated with 11.2 µM/ml QMNPs, (C) treated with 6Gy IR, (D) treated with their combination. Cell population % in each phase was quantified. Data are the mean of three independent experiments

Table 2: The percentage of cells as appeared in each phase of the cell cycle as analyzed by Flow cytometry

Groups Parameter		Control	QMNPs	RT	QMNPs+RT
(Apoptosis) %	Mean ±SD	1.4±0.2	16.7±0.2*	6.2±0.2*	10.4±0.2*, €
	P Value	----	0.001	0.02 0.007	0.001 0.007
G1 %	Mean ±SD	37.7±0.1	47.7±0.1*	38.9±0.1	45.7±0.5*, €
	P Value	----	0.001	0.01	0.001 0.01
S%	Mean ±SD	37.6±0.5	22.5±0.4*	38.1±0.1	24.6±0.5*, €
	P Value	----	0.001	0.001	0.001 0.001
G2/M %	Mean ±SD	19.9±0.1	2.1±0.1*	3.1±0.1*	4.8±0.1*
	P Value	----	0.001	0.001	0.001

*The results are the mean of three independent variables. * is the significant of the treated sets with respect to control set. € is the Significant of QMNPs+RT treated set with respect to RT treatment alone. The P values were presented in the table. NS means Non Significant*

Magnetite nanoparticles have been widely used in biomedicine, as they proved to be stable, non-toxic and non-carcinogenic. Several studies revealed the cellular responses induced by magnetite nanoparticles (MNPs) include DNA damage, oxidative stress, mitochondrial membrane dysfunction and changes in gene expression [44]. Its effect depends on particle size, surface coating, exposure route and exposure duration [45]. The biomedical applications of metallic nanoparticles particularly as dual antitumor agents refer to binding to complex biological molecules in order to improve their effectiveness and biocompatibility [46].

This work reports for the first time the potential applicability of the mycosynthesized of iron oxide (Fe3O4) magnetic nanoparticles (MNPs) and the Fe3O4-quericitin (QMNPs) which have been fabricated through a simple, cheap and reproducible approach. This was achieved by free-cell extract of A oryzae and using FeSO4 as a substrate. FeSO4 contain pure iron oxide with a cubic inverse spinal structure. The UV-Vis spectroscopy, transmission electron microscope (TEM), X-rays diffraction (XRD) and Fourier transform infrared spectra (FT-IR) confirmed the size and shape of the fabricated nanoparticles. Fourier transform infrared spectra (FT-IR) confirmed that these Fe3O4 nanoparticles could be successfully coated with active drug, quercetin. The MNPs and QMNPs were generally spherical, with an average diameter of 11 nm and 40nm, respectively. The funtionalization of surface of the Fe3O4 nanoparticles was obtained by the electrostatically quercetin coating onto the nano biocomposite of the quercetin - Fe3O4 in order to enhance the sensitivity, specificity, stability and reproducibility of the QMNPs. [47,48,49].

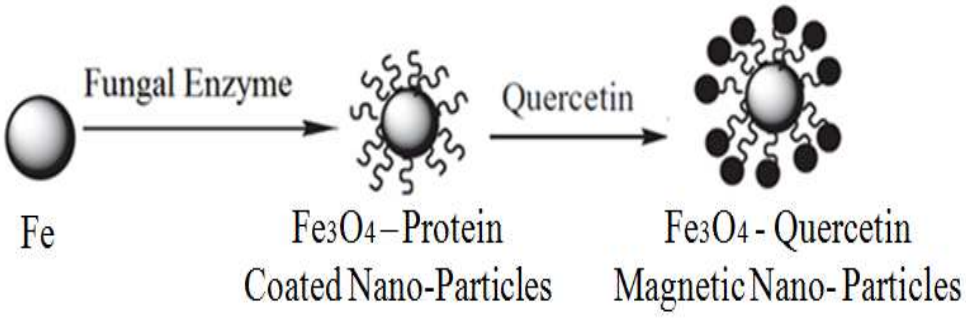

Figure 11: Schematic illustration of the reaction mechanisms for the overall synthesis process of the quercetin loaded Fe3O4 nanoparticles via A.oryzae

In the current study, the enhancement of the cytotoxicity of MCF-7, HepG2 and A459 as in vitro models of human cancer cells by QMNPs was evaluated. The cells were incubated at concentrations of QMNPs in the range of 5–20 nM/ml for 48hrs. The results showed that QMNPs exhibits dose dependant and cell type specific cytotoxicity with IC50 values of 11.2nm/ml, 77.5nm/ml and 104nm/ml for these cells respectively. The results also clearly suggest that the MCF-7 cell lines were the most sensitive towards the formulated QMNPs as its IC50 was 11.2 nm/ml compared with 77.5nm/ml and 104nm/ml for HepG-2 and A459 which could be considered more resistance towards our formulated QMNPs than the MCF-7 cells. The present observations are in agreement with other researchers [50], who testified that QFe3O4NPs showed concentration dependant cytotoxicity. They endorsed this effect to the rapid release rate of quercetin owing to the breakage of ester bond from Fe3O4NPs which interact with particular cancer cells in acidic environment. Thus, it was confirmed that the loss of cell viability could be due to the massive

release rate of the quercetin from QFe3O4NPs. They also concluded that Fe3O4 NPs could be considered as a sustained drug delivery system with quercetin which improved the bioavailability for normal cells but toxic to the cancer cells. The higher toxicity of the breast cancer cells might happen due to the strong binding between the MCF-7 cells and quercetin molecules due to the partial release of quercetin from the magnetite nanoparticles and magnetic oxidation that resulted in DNA damage [30]. Our results clearly indicate the conspicuous therapeutic effect of the QMNPs which greatly enhances the MCF-7 anticancer activity than the other two examined cell lines.

Treatment of cancer by radiation is a most common modality; however, the outcome is limited as healthy tissues in neighborhood of target tumor cells are adversely affected [51]. Clinical studies have demonstrated the benefits of adjuvant radiotherapy for improving disease-free survival, overall survival and local control, and reducing disease recurrence after surgical resection in breast cancer patients [52].

In this study we demonstrated the optimal dose of irradiation (IR) that results in potent cytotoxicity in MCF-7 cell lines. The cells were exposed to 4, 6, 8, and 10 Gy for 24 hr exposure. The sensitivity of MCF-7 cell lines to the different doses of IR was run by MTT assay. Our results revealed variation in the decrease of cell viability after the initial 24 hr of IR exposure. The reduction in the viability was more pronounced in MCF-7 set exposed to 6Gy. Many of in vitro studies have shown that irradiation of MCF-7 cells with various doses has led to different results. Some studies have indicated the decrease in the viability in MCF-cell lines exposed to 1Gy and 4Gy, but the rate of the cell viability decrease was slower than that of 1 Gy X-rays [53]. In consistence with our results, Fazel and fellow-workers demonstrated the viability of MCF-7 cancer cells after exposure to different RT doses (1, 2, 4, 6, 8, 10, 20 Gy). They indicated that the percentage of reduction in cell viability with 6Gy was more obviously than with other doses [54].

The discovery of novel agents which sensitize malignant cells to radiation would increase tumor response, while minimizing toxicity to the surrounding organs by lowering the effective therapeutic dose. In this regard the potential mechanisms by which QMNPs enhanced the irradiation killing effect in MCF-7 cancer cell were further explored by quantifying the antiproliferative effect, the production of ROS and analyzing the early apoptotic cell death and distribution of cell fractions in the different phases of cell cycle in MCF-7 treated with QMNPs and radiation alone or in combination.

The superparamagnetic properties magnetite (Fe_3O_4) is of great important. These proprieties allow them to be directed and localized to a particular organ by using external magnetic force [55]. These are also known to be highly biocompatible with negligible toxicity to healthy tissues allowing for usage in therapy [56]. Scientific findings by Roa and colleagues have shown the Radiosensitization of NPs and induction of cell death in the first 24hr after initial treatments of the cancer cells [57]. In the line with those, our results indicated that QMNPs enhanced irradiation induced the lowering of MCF-7 growth as examined qualitatively by MTT assay. Other studies showed that combination of cytotoxic agent with magnetic NPs in combination with RT resulted in more cell killing and inhibits cell survival consequently cell proliferation was inhibited [58] and induced DNA damage *in vitro* [59]. This effect could be endorsed to the intensifying the production of secondary electrons and ROS that in turn enhance radiation therapy effects by these NPs [60].

Since radiotherapy treatment of tumor cells is associated with enhancing the generation of ROS. Hence one of the main objectives of our study was to quantify and understand the enhancing effect of QMNPs on γ-rays enhanced the formation of ROS in irradiated MCF-7 cells. Our results obviously demonstrated that, QMNPs on its own enhanced the production of ROS and are consistent with other studies reported that Fe3O4 acts as radiosensitizers via enhancing the formation of ROS [39,61] which could be due to the presence of pro-oxidant functional groups on their reactive surface or due to nanoparticle-cell interactions [62]. Other studies evidenced that, quercetin has been described as a pro-oxidant and can induce the production of superoxide anion, hydrogen peroxide, and other reactive oxygen species (ROS) which are responsible for cell death in some cancer cells [63]. Moreover, in our study RT treatment significantly enhanced the production of ROS ($P<0.001$) compared to control set as manifested in our results. In the same line with our observation, the research findings showed that radiotherapy treatment of tumor cells is associated with enhancing the free radical formation [64] which resulted in the generation of ROS. These ROS leads to the damage of biomolecules induce DNA damage and deregulate the apoptotic signaling pathway, ultimately inducing apoptosis [65]. In the current study, the combination of QMNPs and RT treatment could potentiate the enhancing potential of RT treatment to generate the ROS. In agreement with our findings, many investigators reported that most of radiosensitizers can upregulate ROS which is one of the important-mediated mechanism and is considered as a potential target for improving radiotherapy [66-67].

Regarding the effect of the different treatments on the induction of early apoptosis and alter the progression of cell cycle phases of the genomic DNA. The cells were treated with 11.2nM/m of QMNPs and 6Gy γ-rays either alone or

in combination and were analyzed by FCM 24hr post treatment. Our results clearly demonstrated that QMNPs as a sole treatment and in combination with RT caused severe DNA damage and consequently enhanced the induction of apoptosis at sub-G1 phase. Furthermore, the effect of different treatments on cell cycle progression in MCF-7 cells was demonstrated. The data in the present study revealed that QMNPs enhanced G1/G0 growth arrest and significantly augment the enhanced RT-induced G1 growth arrest and reduced S-phase synthesis of DNA. Our results are consistent with previous reports which showed that since NPs are able to penetrate cells [67] into cell nuclei and hence may directly interfere with the structure and function of genomic DNA and can also interfere with several sub-cellular mechanisms [68] depending on their small diameter which does not exceed a hundred nanometers at maximum. As previously reported quercetin has been demonstrated to play an important role as a pro-apoptotic inducer and blocks the growth of several human cancer cells at different phases of cell cycle [69]. Other research results have indicated that metal oxide NPs exhibit a dose-dependent effect on specific phases of the cell cycle owing to the activation of metabolic stress pathways [70,71]. In a late study, it has been emphasized that QNPs exhibited obvious anticancer effect towards cancer cells and has the potential to interact with DNA which caused inhibition of the normal synthesis of DNA at some levels and made it to induce apoptosis [72]. Moreover, the interaction with DNA increased the capability of the drug to inhibit cell proliferation and induce cell cycle arrest [73-74].

CONCLUSION

Altogether, the findings of this study conclude that QMNPs was successfully synthesized biologically which mediated by *Aspergillus Oryazae.* The formulated QMNPs displayed concentration dependant and cell specific cytotoxicity. Its radiosensitization towards MCF-7 cells was clarified through enhancing the inhibition of cell proliferation, abrogating the generation of ROS and augmenting the DNA damage and induction of early apoptosis in sub-G1 phase, altering the progression of cell cycle phases and arrested the cells at G0/G1 phase. Thereby, sensitize the cells to RT and finally enhanced the apoptotic cell death. Further analysis must be required to confirm the antitumor activity of QMNPs and to explore the mechanisms of action responsible for its capability to enhance the radiosensitivity in vivo.

REFERENCES

[1] HD Xiao; YS Hai; FZ Ying; et al, *Exp Ther Med*., **2016**, 6 (5): 1155–1158.
[2] World Health Organization. Global Health Estimates [Internet]. **2012** [cited July 9, **2014**]. Available online.
[3] M Tubiana; J Dutreix and A Wambersie, *Medical Physics*., **1992**, 62 (1): 125.
[4] K Kobayashi; N Usami; E Porcel; et al, *Mutation Research/Reviews in Mutation Research.*, **2010**, 704 (1-3):123-131.
[5] TB Karl; JM Stephen; JC Fred; et al, *Nanoscale*., **2012**, 4: 4830-4838.
[6] IB Ross; N Wilfred and MG Makrigiorgos, *Radiation Oncology*., **2011**, 81 (1): 270-276.
[7] SJ McMahon; MH Mendenhall; S Jain; et al, *Phys Med Biol*., **2008**, 53 (20): 5635-51.
[8] M Misawa and J Takahashi, *Nanomedicine: Nanotechnology, Biology and Medicine.*, **2011**, 7(5): 647-654.
[9] F Geng; K Song; J Xing; et al, *Nanotechnology*., **2011**, 22 (28): 285101-285108.
[10] M Ott; V Gogvadze; S Orrenius; et al, *Apoptosis*., **2007**, 12 (5): 913-22.
[11] P Poortmans, *European Journal of Cancer Supplements.*, **2013**, 11 (2): 27–36.
[12] MS Wason; J Colon; S Das; et al, *Nanomedicine: Nanotechnology, Biology, and Medicine.*, **2013**, 9 (4):558 - 569.
[13] PD Ray; BW Huang and Y Tsuji, *Cellular Signalling*., **2012**, 24 (5): 981–990.
[14] SA Quast; A Berger and Eberle J, *Cell Death & Disease*., **2013**, 4 (10, article e839):13.
[15] JH Sherman; J Kirzner; A Siu; et al, *Journal of Clinical Neuroscience*., **2014**, 21 (1): 131–136.
[16] L Agoni; I Basu; S Gupta; et al, *International Journal of Radiation Oncology Biology Physics*., **2014**, 88 (5): 1180–1187.
[17] T Oike; M Komachi H Ogiwara; et al, *Radiotherapy and Oncology*., **2014**, 111 (2):222–227.
[18] FH Sarkar; Y Li; Z Wang; et al, *Curr Pharm Des*., **2010**, 16 (16):1801-12.
[19] MM Yallapu; Meena Jaggi and CC Subhash, *Curr Pharm*., **2013**, 19 (11): 1994–2010.
[20] G Lara; P Marcello; N Milena; et al, *Evidence-Based Complementary and Alternative Medicine*., **2011**, (2011): 591356 (15).
[21] M Russo; S Carmela; T Idolo; et al, *Biochemical Pharmacology*., **2012**, 83 (1): 6-15.
[22] L Ma; JM Feugang; P Konarski; et al, *Front Biosci*., **2006**, 1 (11): 2275-85.
[23] RG Beniston and MS Campo, *Oncogene*., **2003**, (22): 5504–5514.
[24] C Lin; Y Yu; HG Zhao; et al, *Radiother Oncol*., **2012**, 104 (3): 395-400.
[25] JP Patel; M Gönen; ME Figueroa; et al, *N Engl J Med*., **2012**, 366 (12):1079-89.
[26] M Kumari; B Ellena; S Amanda; et al, *Psychoneuroendocrinology*., **2010**, 1749: 9.
[27] JH Park; S Lee; JH Kim; et al, *Prog. Polym. Sci*., **1998**, 33 (1), 113–137.
[28] VV Makarov; AJ Love; OV Sinitsyna; et al, *Acta Naturae*., **2014**, 6 (1): 35-44.

[29] I Maliszewska; A Juraszek; and K Bielska; *J Clust Sci*., **2014**, 25: 989-1004.
[30] KS Siddiqi and H Azamal, *Scope and Application Nanoscale Res Lett*., **2016**, 11: 98.
[31] S Azarmi; WH Roa; and Lobenberg R, *Adv Drug Deliv Rev*., **2008**, 60: 863-875.
[32] S Akhter; S Amin; J Ahmad; et al, *Springer International Publishing*., **2015**, 245-272.
[33] S Akhter; I Ahmad; MZ Ahmad; et al, *Curr Cancer Drug Targets*., **2013**, 13 (4): 362–378.
[34] SA Krishna; P Amareshwar and HD Jayapraka, *International J of Pharmacy and Integrated Life Sciences*., **2013**, 1(3): 69-75.
[35] R Protima; K Siim; F Stanislav; et al, *Advances in Materials Science and Engineering*., **2015**, 9.
[36] J Conde; TD Jorge; G Valeria; et al, *Front Chem*., **2014**, 2: 48.
[37] A Kumar; M Mazzanti; M Mistrik; et al, *Cell*., **2014**, 158 (3): 633-46.
[38] E Joan; JS María and AB Maria, *Int J Nanomedicine*., **2015**, **10**: 1727–1741.
[39] R Khonkarn; S Mankhetkorn; WE Hennink; et al, *Eur J Pharm Biopharm*., **2011**, 79: 268–275.
[40] K Kathiresan; S Manivannan; MA Nabeel; et al, *Colloids Surf B Biointerfaces*., **2009**, 71 (1):133-7.
[41] MB Hansen; SE Nielsen and K Berg, *J. Immunol. Methods*., **1989**, 119: 203-10.
[42] VK Stefka; B Branka and V Srećko, *Pharmacogn Mag*., **2012**, 8 (30): 171–174.
[43] F Jhi Biau; SY Latifah; ST Yin; et al, *BMC Complement Altern Med*., **2014**, 14: 197.
[44] N Singh; GJS Jenkins; R Asadi; et al, *Nano reviews*., **2010**, (1): 1-15.
[45] S Klein; A Sommer; LV Distel; et al, *Biochem Biophys Res Commun*., **2010**, 425: 393-7.
[46] VRP Pasupuleti; RA Shiekh; SK Balam; et al, *Int J Nanomedicine*., **2013**, 8: 3355-64.
[47] B Atul; R Debabrata; B Vipul; et al, *Small*., **2006**, 2 (1): 135-141.
[48] N Durán; M Priscyla; AL Oswaldo; et al, *Journal of Nanobiotechnology*., **2005**, 13: 3-8.
[49] Zhiqiang Wang, *ACS Sustainable Chem. Eng.*, **2013**, 1 (12): 1551–1554.
[50] S Laurent and M Mahmoudi, *Int J Mol Epidemiol Genet*., **2011**, 2(4): 367–390.
[51] Wang Shibin and S Gaoquan, *Materials Chemistry and Physics*., **2007**, 102 (2-3): 255–259.
[52] D Renu; PM Kaushala; P Anubhuti; et al, *Journal of Cancer Research and Therapeutics*., **2014**, 10 (4): 811-818.
[53] H Bartelink; JC Horiot; PM Poortmans; et al, *J Clin Oncol*., **2007**, 25(22):3259-65.
[54] YL Wang; H Zhang; N Li; et al, *Nuclear Instru and methods in physics Res*., **2009**, 267:1001-6.
[55] S Fazel; Z Chang; T Fanshawe; et al, *Lancet Psychiatry*., **2016**, 3(6):535-43.
[56] AS Wadajkar; JU Menon; T Kadapure; et al, *Recent Pat Biomed Eng.*, **2013**, 6: 47-57.
[57] G Mikhaylov and O Vasiljeva, *Biol Chem*., **2011**, 392: 955-60.
[58] W Roa; X Zhang; L Guo; et al, *Nanotechnology*., **2009**, 20:375101.
[59] JA Coulter; S Jain; KT Butterworth; et al, *Int J Nanomedicine*., **2012**, 7: 2673–85.
[60] G Huang; H Chen; Y Dong; et al, *Theranostics*., **2013**, 3: 116-26.
[61] P Retif; P Sophie; T Magali; et al, *Theranostics*., **2015**, 5(9): 1030–1044.
[62] A Sarkar; M Ghosh and PC Sil, *J. Nanosci. Nanotechnol*., **2014**, 14: 730–743.
[63] L Risom; P Møller and S Loft, *Mutat. Res*., **2005**, 592: 119–137.
[64] B Halliwell, *Arch Biochem Biophys*., **2008**, 476 (2):107–112.
[65] L Zhang; M de-Waard; H Verheijen; et al, *Data Brief*., **2016**, (7): 362-5.
[66] HJ Sherman; J Kirzner; A Siu; et al, *J. of Clinical Neuroscience*., **2014**, 21 (1): 131–136.
[67] LI Agoni; S Basu; S Gupta; et al, *Int J Radiat Oncol Biol Phys*., **2014**, 88(5): 1180–1187.
[68] K Park, *J Control Release.*, **2007**, 120 (1-2): 1–3.
[69] M Chen and A Von Mikecz, *Exp Cell Res*., **2005**, 305 (1): 51-62.
[70] HY Jung; J Heo; Y Lee; J et al, *Life Sciences*., **2010**, (86): 351–357.
[71] S Hussain; CTF Leen; Ioana; et al, *Part Fibre Toxicol*., **2010**, **7**: 10.
[72] J Athinarayanan; SP Vaiyapuri; AA Mohammed; et al, *Cell B. Toxicol*., **2014**, 30 (2):89-100.
[73] K Bishayee; RA Khuda-Bukhsh and Sung-Oh Huh, *Mol Cells*., **2015**, 38 (6): 518–527.
[74] SC Devi; KD Anil; SS Singh; et al, *Eur J Med Chem*., **2013**, 64: 410-21.